Desalination and Water Treatment
www.deswater.com
doi: 10.1080/19443994.2013.827292

52 (2014) 570–579
January

Taylor & Francis
Taylor & Francis Group

Removal of dissolved organics from produced water by forward osmosis

Rajab M. Abousnina, Long D. Nghiem*

Strategic Water Infrastructure Laboratory, School of Civil Mining and Environmental Engineering, University of Wollongong, Wollongong 2522, Australia
Tel. +61 2 4221 4590; email: longn@uow.edu.au

Received 23 February 2013; Accepted 18 March 2013

ABSTRACT

This study investigated the performance of the forward osmosis (FO) process for treating produced water. Water permeate flux and reverse salt flux (RSF) were examined at different feed pH values and operating configurations (i.e. FO, pressure retarded osmosis (PRO), and reverse osmosis (RO) modes). Acetic acid was selected as a model organic acid to present the dissolved organic fraction in produced water. Results reported here indicate that only membranes specifically designed for FO applications can be used in the FO and PRO modes. Due to the internal concentration polarization phenomenon, the PRO mode resulted in a higher water permeate flux and RSF than those in the FO mode. Acetate rejection was pH dependent in both the FO and RO modes. Furthermore, in the RO mode, acetate rejections by the FO membranes were higher than their nanofiltration counterparts. Results reported here suggest that FO can be a viable treatment option for the removal of dissolved organics from produced water.

Keywords: Produced water; Forward osmosis; Oily wastewater; Acetic acid; Dissolved organics

1. Introduction

Produced water is water extracted from underground formations and brought to the surface during the production of either oil or gas. It is considered to be the largest by-product or waste stream (by volume) associated with the production of oil and gas, and as such it is a major source of many pollutants and can pose a considerable threat to the environment. It has been reported that inappropriate disposal of untreated produced water may lead to severe adverse effect to the ecosystem including various plant and aquatic species [1–3]. In addition, contaminated soil can lead to wide spread contamination of surface water and shallow aquifers. The US Environmental Protection Agency (US-EPA) has recognized the potential impact of the disposal of produced water on the environment and have stipulated set regulations for controlling the amount of mineral oil and other associated contaminants [4].

The volume of produced water is not constant over time and the ratio of water to oil or gas increases over the lifetime of the oil or gas well. Water initially makes up a small percentage of fluids when a well is new, whereas over time the volume of water tends to

*Corresponding author.

Presented at the Fifth Annual International Conference on ''Challenges in Environmental Science & Engineering—CESE 2012'' Melbourne, Australia, 9–13 September 2012

increases as the product yield declines. The estimated average global production of produced water is 210 million barrels (bbl) per day, resulting in an annual estimation of 77 billion bbl per year [4]. The volume of produced water has increased dramatically over the last few decades as more oil and gas reservoirs are being exploited in areas where extraction is difficult. Produced water contains a large number of dissolved organic compounds such as hydrocarbons, organic acids, phenols, and BTEX (which is a mixture of benzene, toluene, ethylbenzene, and xylene). Some of these components are toxic to the environment and the concerns with substances such as these components involve toxicity, and due to the complexity of removing components such as these, which end up being discharged into the sea. These components in produced water signify the importance of research in terms of eliminating these components from those sources.

Several studies have been conducted to develop suitable technologies for the treatment of produced water [5–12]. Treatment processes such as oxidation, extraction, stripping, sorption, biological treatment, and membrane technologies have been widely investigated. Membrane processes such as microfiltration (MF), ultrafiltration (UF), nanofiltration (NF), and reverse osmosis (RO) are being used to treat oily wastewater [13–15]. These are pressure-driven filtration processes and thus they are prone to fouling caused by the high oil content of produced water. In addition, while low pressure-membrane processes such as MF and UF are not effective for the removal of dissolved contaminants in produced water, high-pressure processes, such as NF and RO, can be very energy intensive. An alternative to the current treatment technologies is forward osmosis (FO) which is an emerging process that can be effective for the removal of organic contaminants from the aqueous phase [16]. The FO process relies on the osmotic gradient between the feed and draw solutions for the transport water. Thus, when a source of draw solution such as seawater is readily available, the FO process may require very little energy input [17]. Other advantages of the FO process include low fouling tendency and easy fouling removal [18–20], high water recovery [21], and high rejection of a wide range of contaminants [16]. Therefore, the aim of this study is to evaluate the use of FO membranes for the removal of dissolved organics from produced water.

2. Materials and methods

2.1. FO membranes

Two commercially available FO membranes, namely HTI-Cartridge and HTI-Pouch, were acquired from Hydration Technologies Innovation. The former is used in spiral wound (cartridge) membrane modules, and the latter is used for emergency water filter devices such as X-pack and Life-pack (www.htiwater.com). The HTI-Cartridge membrane is made of cellulose triacetate (CTA), which is supported by an embedded polyester screen mesh [16]. The HTI-Pouch membrane is also made of CTA cast onto a nonwoven backing consisting of polyester fibers individually coated with polyethylene, the backing can be heat welded or RF (radiofrequency) welded. Further details about these FO membranes are available elsewhere [16,22]. Two commercially available NF membranes, namely NF-270 and NF-90, supplied by Dow Chemical were also selected for this study for comparison with the FO membranes. The characteristics of these NF membranes are described in details elsewhere [23].

2.2. FO and RO experimental systems

The experiment was conducted using a closed loop bench-scale FO membrane system, as shown in Fig. 1. The channel is 14.5 cm long by 9.5 cm wide by 0.2 cm deep, the membrane cell is made from acrylic plastic, and its total effective area for mass transfer is 135.82 cm^2.

To circulate the feed and draw solutions, two variable speed gear pumps (Micropump, Vancouver, WA) were used. Flow rates of the feed and draw solution flow were monitored using two rotameters and kept constant at 1 L/min. A computerized system was used to maintain a constant draw solution concentration throughout the experiment. The draw solution tank is placed on a digital scale (Mettler Toledo Inc.), and any changes in weight are transmitted by a computer to get the permeate flux. The conductivity of the draw solution is continuously measured with a conductivity probe. The peristaltic pump is controlled by a conductivity controller to occasionally pump a small volume of highly concentrated NaCl draw solution (6 M) into the draw solution tank to maintain a constant concentration of draw solution. The tank of concentrated draw solution is attached to the draw solution on the same digital balance to avoid any interference when measuring the permeate flux between the two tanks during these processes.

A laboratory scale-NF/RO filtration system was used to conduct RO mode experiments. The system consisted of a stainless steel cross-flow cell, a digital flow-meter, a high-pressure pump, and a temperature control unit. Detailed description of this system is available elsewhere [24].

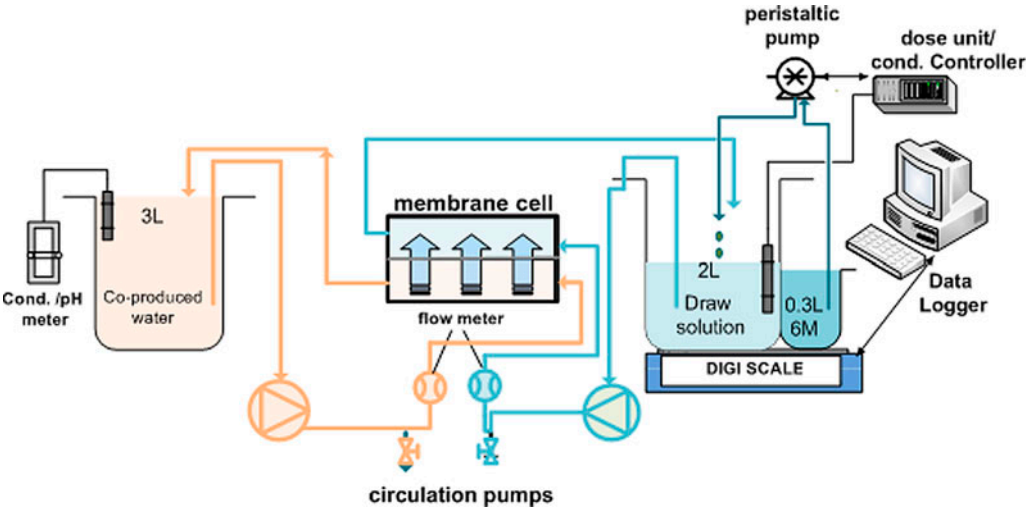

Fig. 1. Schematic diagram of FO system.

2.3. Experimental protocol

Acetate (CH_3COO^-) was selected as a model dissolved organics to represent organic acids that occur widely in produced water. Concentration of acetate in the feed solution was 300 mg/L, which on average represents the total concentration of organic acids often found in produced water. When required, HCl (1 M) or NaOH (1 M) were used to adjust the initial pH value of the feed solution to pH 6, 4 and unadjusted pH (6.7–7.3), respectively. The initial volumes of the feed and draw solutions were 3 L and 2 L, respectively. The draw solution used for all experiments was 0.5 M NaCl. The temperature of the feed and draw solutions was monitored under a room temperature of 25 ± 2°C. A new FO membrane coupon was used for each experiment. Approximately, 1 mL samples were taken from both the feed and draw solutions at specific time intervals, for acetate analysis. In this study, the configuration in which the feed solution was in contact with the active layer of the FO membrane was defined as the FO mode. The configuration in which the draw solution is in contact with the membrane active layer is defined as the pressure retarded osmosis (PRO) mode.

In the FO process, the permeate concentration of target solute is diluted by the draw solution and the apparent concentration of the target solute in the draw solution cannot be directly used to calculate the rejection value. Thus, to evaluate the real performance of the FO process, the actual (corrected) concentration of the target solute, $C_{s(t)}$ is recalculated by taking the dilution into account using mass balance:

$$C_{s(t)} = \frac{C_{ds(t)}V_{ds(t)} - C_{ds(t-1)}V_{ds(t-1)}}{V_{w(t)}} \quad (1)$$

where $V_{w(t)}$ is the permeate volume of water to the draw solution at time t, $V_{ds(t-1)}$ is the volume of draw solution at time $(t-1)$, $V_{ds(t)}$ is the volume of draw solution at time t, $C_{ds(t)}$ is the measured concentration of target solute in the draw solution at time t, and $C_{ds(t-1)}$ is the measured concentration of target solute in the draw solution at time $(t-1)$. Subsequently, the solute rejection in the FO process is calculated using the actual (corrected) permeate concentration, yielding:

$$R_{FO} = \left(1 - \frac{C_{s(t)}}{C_{f(t)}}\right)100\% \quad (2)$$

where $C_{f(t)}$ is the concentration of the target solute in the feed at t time.

Rejection by in RO mode was calculated as $R = 100 \times \left(1 - \frac{C_p}{C_f}\right)$, where C_p and C_f are the concentration of target solute in the permeate and feed solution, respectively. The reverse flux of the draw solute was determined using the mass balance calculation as, $J_{salt} = \frac{C_tV_t - C_0V_0}{At}$ where C_0 and C_t are the concentration of the draw solute in the feed at 0 and t time, respectively; V_0 and V_t are the volume of the of the feed at 0 and t time, respectively; A is the membrane area. The concentration of NaCl in the feed solution was determined by conductivity measurement based on a linear relationship between conductivity and NaCl concentration.

2.4. Analytical methods

Acetate concentration was determined using a Shimadzu Ion Chromatography system. The system consisted of two LC-20AD pumps, a model DGU-20A3 degasser unit, a SIL-20A auto sampler (a CTO-20A thermostatic column model AS23). The column temperature was maintained at 35°C by a CTO-20A column oven. To minimize any interference from the background matrix, standard solutions were prepared in 0.5 M NaCl. A linear calibration curve was obtained with R^2 value of 0.99. pH and conductivity were measured using an Orion 4 Star pH and conductivity meter.

2.5. Zeta potential measurement

Zeta potential (ζ) of the membrane surface was measured using a SurPASS electrokinetic analyzer (Anton Paar GmbH, Graz, Austria). The zeta potential of each membrane surface was calculated from the measured streaming potential using the Fairbrother–Mastin approach. All measurements of the streaming potential were conducted in a background electrolyte solution containing 10 mM KCl. Hydrochloric acid and sodium hydroxide was used to adjust the pH. The test solution was used to thoroughly flush the cell prior to the pH adjustment for each measurement. All measurements of the streaming potential were performed at a room temperature of approximately 25°C, which was monitored by the temperature probe inside the instrument.

2.6. Contact angle measurement

Contact angle measurements were conducted using a Rame-Hart Goniometer (Model 250, Rame-Hart, Netcong, NJ) following the standard sessile drop method. Prior to the contact angle measurement, the membrane samples were dried in a desiccator for at least 24 h. To avoid shrinkage, the FO membrane samples were first fixed on to a glass slide using double-sided adhesive tape before drying. On the other hand, the NF membrane samples did not require any special pretreatment. Ten water droplets were used on each membrane sample and contact angles on both sides of the droplet were analyzed.

3. Results and discussion

3.1. Membrane characterization

The four membranes selected in this study differ from one another in their polymeric composition and internal structure in that the HTI-Pouch and HTI-Cartridge membranes are made of CTA. According to the manufacturer, the HTI-Pouch is a thin-film composite membrane with a thin layer of CTA fused onto a layer of nonwoven polyester fiberthat is individually coated with polyethylene. On the other hand, the HTI-Cartridge is a polyester screen mesh embedded within an asymmetric layer of CTA [25]. Both the NF-90 and NF-270 are thin-film composite membranes with an ultra-thin layer of polyamide skin on top of a supporting layer of microporous polysulfone. Given the difference in their polymeric composition and internal structure, their physiochemical properties and performance also differs, and hence, their intrinsic separation properties are also expected to be different.

The water permeability (A value) and salt (NaCl) permeability (B value) were measured according to the standard protocol recently proposed by Cath et al. [26]. The NaCl rejection of the selected membranes was as follows: HTI-pouch > HTI-cartridge > NF-90 > NF-270 (Table 1), which is consistent with the B value of the selected membranes. The NF-270 is considered to be a loose NF membrane with a low rejection of sodium whereas the NF-90 is a tight NF membrane with moderate rejection of sodium (Table 1). The HTI membranes have slightly larger pores than the NF-90 membrane and smaller pores than the NF-270 membrane. It is noteworthy that both

Table 1
Properties of the selected membranes

Membrane	Water permeability A ($Lm^{-2}h^{-1}bar^{-1}$)	NaCl permeability B ($L\ m^{-2}\ h^{-1}$)	NaCl retention (%)	Contact angle (°)	Average pore diameter[a] (nm)
HTI-Pouch	0.745	0.083	95–97	65	0.70
HTI-Cartridge	1.13	0.64	93–95	64	0.74
NF-90	6.4	1.32	85.0	51	0.68
NF-270	19.29	34.11	40.0	29	0.84

[a]Refs. [24,27].

HTI membranes have much lower *A* and *B* values compared with the NF-90 and NF-270 membranes (Table 1).

The results of the contact angle measurements show that all the membranes used are hydrophobic, except the NF-270. The hydrophobicity of both NF membranes is less than the HTI FO membranes. The surface charge of the selected membranes is pH-dependent, as the pH increases the membranes become more negatively charged (Fig. 2). Therefore, the electrostatic interaction between the charged organic solutes and the surface of the charged membrane can influence the rejection of organics. Studies on electrostatic interaction have reported that an increase in the rejection of negatively charged organic solutes resulted from an electrostatic repulsion between the negatively charged membrane and the negatively charged organic solute [28–29]. This rejection, however, is based on the initial feed pH, since both the surface change on the surface of the membrane and the organic solute vary according to the pH (through a dissociation of the functional groups as a function of their p*K*a).

It has been reported that a more negative zeta potential could lead to a higher rejection of salt due to an enhanced electrostatic interaction between the negatively charged surface of the membrane and a negatively charged solute [30]. The zeta potential of the surface of the membrane varies as a function of the solution pH (Fig. 2). The zeta potential of the membrane in the HTI-Cartridge membrane is not as sensitive to pH as the HTI Pouch. The active and backing layers of the HTI-Cartridge membrane show an almost identical zeta potential profile as a function of pH, while there is a notable difference in the zeta potential profile between the active and backing layers of the HTI Pouch membrane. These results are consistent with the difference in structure of the HTI Cartridge and Pouch membranes as described previously. Both the NF-270 and NF-90 membranes are much more negatively charged compared with the HTI membranes particularly at above neutral pH. Results reported here suggest that the active skin layers of the two polyamide NF membranes contain significantly more ionizable functional groups than those of the cellulose acetate HTI membranes.

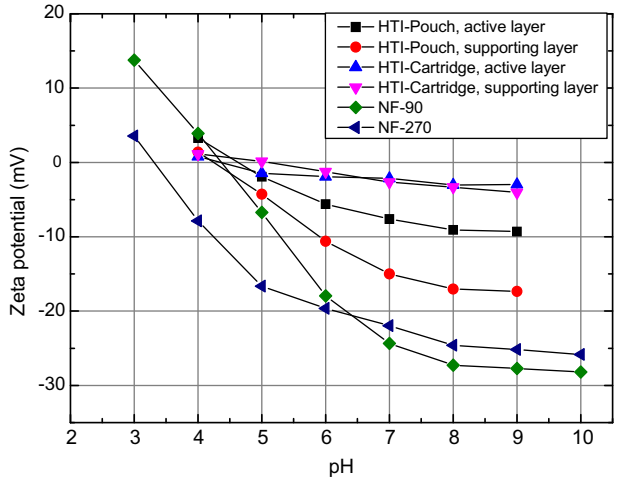

Fig. 2. Zeta potential of the selected membranes.

3.2. General behavior of the FO process

3.2.1. Water flux and reverse salt flux

Despite having significantly higher *A* and *B* values than the two FO membranes selected in this study, the NF-90 and NF-270 did not produce any permeate flux when they are operated under the FO mode. Therefore, only the water fluxes as a function of time obtained from the HTI-Cartridge and HTI-Pouch membranes under the FO mode are presented in Fig. 3. Because the draw solution concentration was constant, the water permeate flux was stable throughout the experiment. Under the same operating condition, the water permeate flux by the HTI-Cartridge membrane was considerably higher than that by the HTI-Pouch membrane (Fig. 3). This is because the HTI-Cartridge membrane has a larger pore size than that of the HTI-Pouch membrane (Table 1). Additionally, these results are also consistent with the pure water permeability (A value) of these two FO membranes (Table 1). The effect of the initial feed pH in the range from pH 4 to 7.3 on the water permeate fluxes by these two FO membranes under the FO mode was insignificant (Fig. 3).

Mass transport in the FO process can be bi-directional [31], and the leakage of salts (or reverse salt flux (RSF)) can occur with a nonidealized membrane. This RSF is measured by monitoring the increase in conductivity in the feed solution using a calibration curve for the NaCl solution as described in Section 2.3. Fig. 4 shows the reverse NaCl fluxes obtained with the HTI-Cartridge and HTI-Pouch membranes under different initial feed solution pH, namely un-adjusted pH (6.8–7.3), 4, and 6, respectively. The effect of feed solution pH on the RSF by both the HTI-Cartridge and HTI-Pouch membranes was also insignificant (Fig. 4), similar to the observation regarding the water flux (Fig. 3). The reverse NaCl fluxes observed with the HTI-Cartridge membrane were significantly higher than those observed with the HTI-Pouch membrane (Fig. 4). This observation of the RSF is again in a good

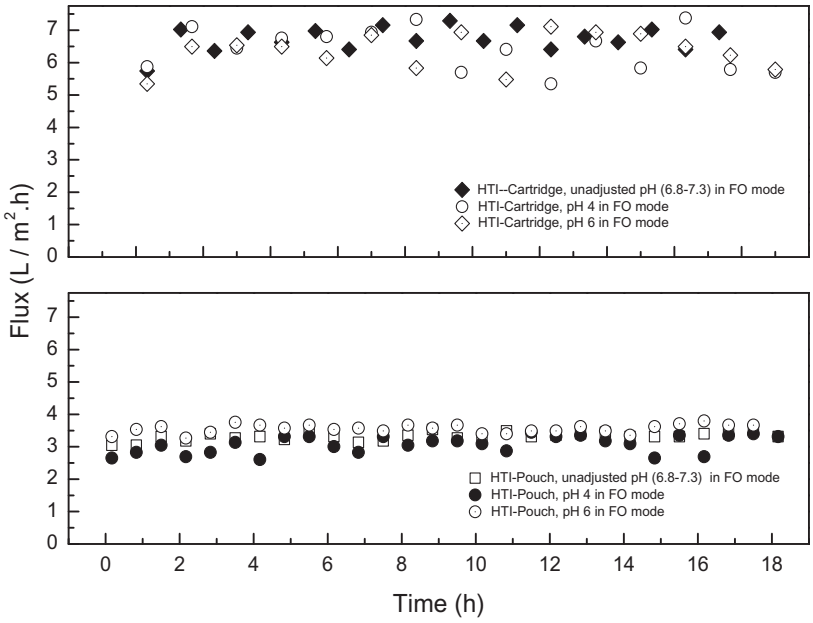

Fig. 3. Water flux as a function of time at different pH values of the feed in the FO mode (draw solution = 0.5 M NaCl, cross-flow rate = 1 L/min for both sides, and cross-flow velocity = 9 cm/s).

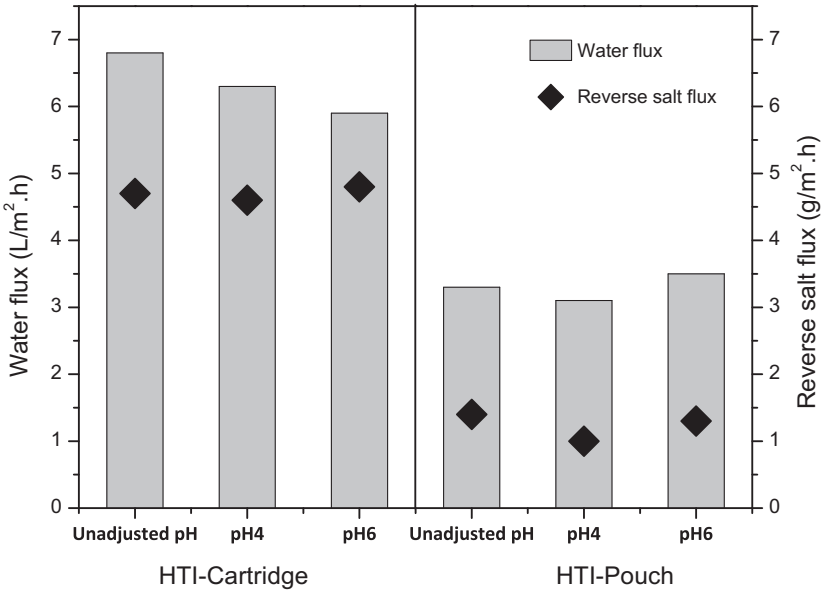

Fig. 4. Water and RSFs of NaCl of the HTI-Cartridge and HTI-Pouch membranes.

agreement with the *B* value (salt permeability) of these two membranes as previously discussed in Section 3.1.

3.2.2. Effects of membrane orientation

Of the two FO membranes used in this study, the HTI-Cartridge membrane shows a significantly higher water flux. Thus, it was selected for further investigation to evaluate the impact of the membrane orientation on water flux and RSF.

The HTI-Cartridge membrane was used in both the FO and PRO modes using the laboratory FO system described previously in Section 2.2. Four experiments were conducted to evaluate the effects of the membrane orientation on the water flux and RSF. Two values of pH were investigated, un-adjusted pH (which was from 6.7 to 7.3) and pH 4.

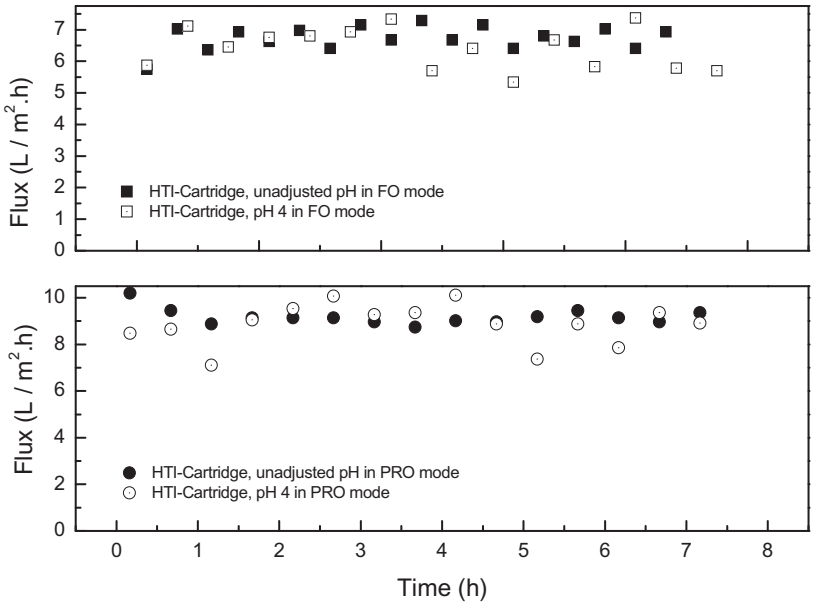

Fig. 5. Water flux as a function of time at different pH values of the feed in the FO and PRO modes. (Initial concentration of acetate in the feed = 300 mg/L, draw solution = 0.5 M NaCl, cross-flow rate = 1 L/min for both sides, and cross flow-velocity = 9 cm/s).

Fig. 5 shows the water fluxes as a function of time when the FO membranes were investigated under the FO mode (i.e. the active layer of the membrane facing the feed solution and the backing layer facing the draw solution), and in the PRO mode (i.e. the backing layer facing the feed solution and the active layer facing the draw solution). The water permeate fluxes obtained under the PRO mode were higher than those obtained under the FO mode. The higher flux obtained under PRO mode was due to the internal concentration polarization (ICP) which considered as a unique phenomenon in FO membranes. When a composite or asymmetric membrane consisting of a dense active layer and porous supporting layer is used in FO, two ICP phenomena can occur, depending on the orientation of the membrane. If the porous support layer on the FO membrane faces the feed solution, a polarized layer is established along the inside of the dense active layer and solute propagates to the porous layer. Referred to as concentrative internal CP [32–33], this phenomenon is similar to the concentrative external CP, except that it takes place within the porous layer and cannot be minimized by cross flow. When the feed solution is against the active layer and the draw solution is against the supporting layer, the ICP phenomenon occurs on the permeate side. It is referred to as dilutive ICP, because the draw solution is diluted by the permeate water within the porous support of the membrane.

The effects of the membrane orientation on the RSF are shown in Fig. 6. The RSF obtained under the FO mode was consistently less than those obtained under the PRO mode which is consistent with the results previously obtained by Xie et al. [34].

3.3. Solute separation

Fig. 7 shows the rejection of acetate by the two FO membranes in the FO mode and by all four membranes in the RO mode. The solution pH appears to be a major parameter governing the rejection of acetate by the membranes selected in this study. These results can be explained by the intricate relationship between the speciation of acetate, membrane surface charge, and solution pH. Acetate can speciate from a neutral species to a negatively charged acetate ion as the solution pH increases beyond its p*K*a value of 4.7. In addition, an increase in the solution pH can also increase the membrane negatively surface charged density (Fig. 2), leading to an enhanced electrostatic interaction with charged solute [30].

Results reported in Fig. 7 systematically demonstrate the significance of electrostatic interaction and the major rejection of acetate by the HTI-Cartridge and HTI-Pouch FO membranes under the FO mode. Similar results were obtained by the FO membrane at a high pH value of 6–9 under the RO mode. It is also noteworthy that the rejection of acetate decreased gradually as the pH value of the feed solution decreased. A much more dramatic decrease in the rejection of acetate occurred with the NF membranes (NF-90 and NF-270) compared to the other two FO

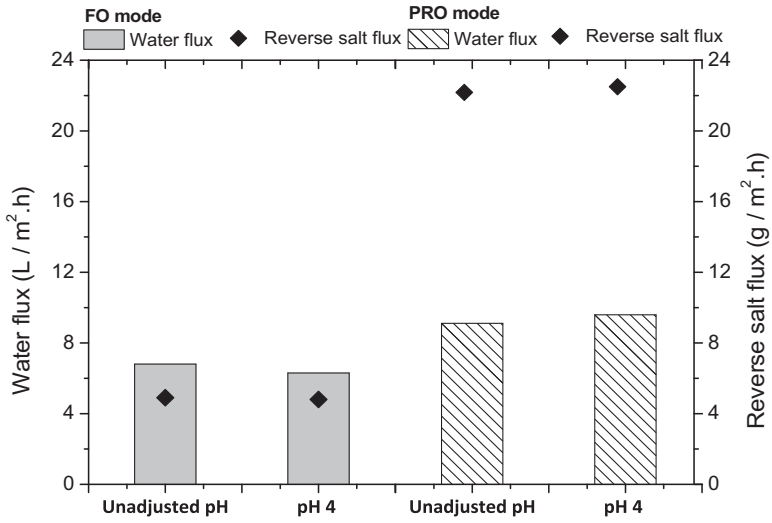

Fig. 6. RSF of NaCl for HTI-Cartridge membrane in the FO and PRO modes.

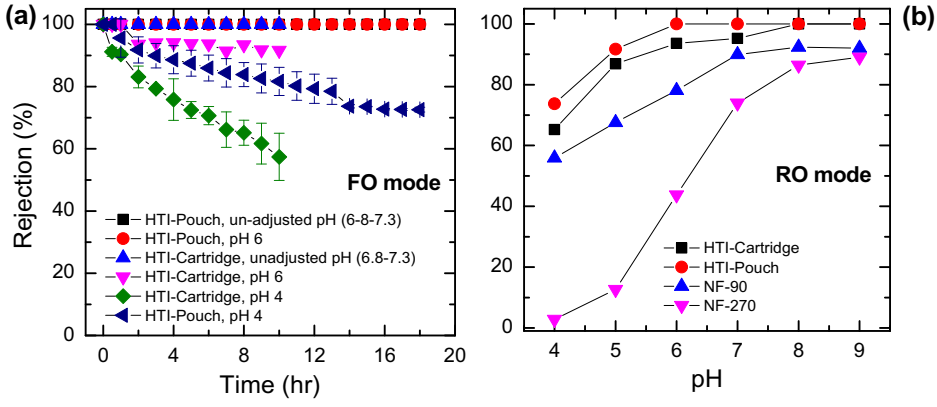

Fig. 7. (a) Rejection of acetate as a function of time at different pH values of the feed in the FO mode; and (b) RO mode rejection of acetate as a function of pH at the same permeate water flux, feed concentration, and temperature. The FO experimental conditions were as follows: The initial concentration of acetate in the feed = 300 mg/L, draw solution = 0.5 M NaCl, cross- flow rate = 1 L/min for both sides, and cross-flow velocity = 9 cm/s, temperature = 25 ± 2°C. The RO experimental conditions were as follows: Initial concentration of acetate in the feed = 300 mg/L, water flux = 8 L/m^{2}h, cross- flow rate = 1 L/min, cross- flow velocity = 25 cm/s, temperature = 25 ± 2°C.

membranes (Fig. 7(b)). Results reported in Fig. 7 suggest that charged repulsion is a predominant rejection mechanism of acetate at high pH. Furthermore, there is a considerable scope for using the FO membrane for the removal of acetate and other dissolved organic acids in produced water. At pH 6 and un-adjusted pH, the rejection of acetate by the FO membranes (HTI-Cartridge and HTI-Pouch) varied from 92 to 100%. Under the RO mode, acetate rejection of 90 to 100% could be achieved with these two FO membranes. With the NF membranes, size exclusion is always an underlying rejection mechanism. The importance of size exclusion is shown by differences in the rejection of acetate at a certain pH. At any given pH value, the rejection of acetate by NF membranes generally increases as the membrane pore size decreases (Fig. 7 and Table 1). It is noted that the rejection of acetate by the NF membranes was less than the HTI-FO membranes, even though that zeta potential of the two HTI FO membranes was less negatively charged than the NF membranes (Fig. 2). In addition, the pore sizes of the FO membranes are intermediate between those values of the NF-90 and NF-270 (Table 1).

The rejection of conductivity in the RO mode was measured every one hour and a relationship between the rejection of conductivity and pH value was established for each experiment. Fig. 8 shows the

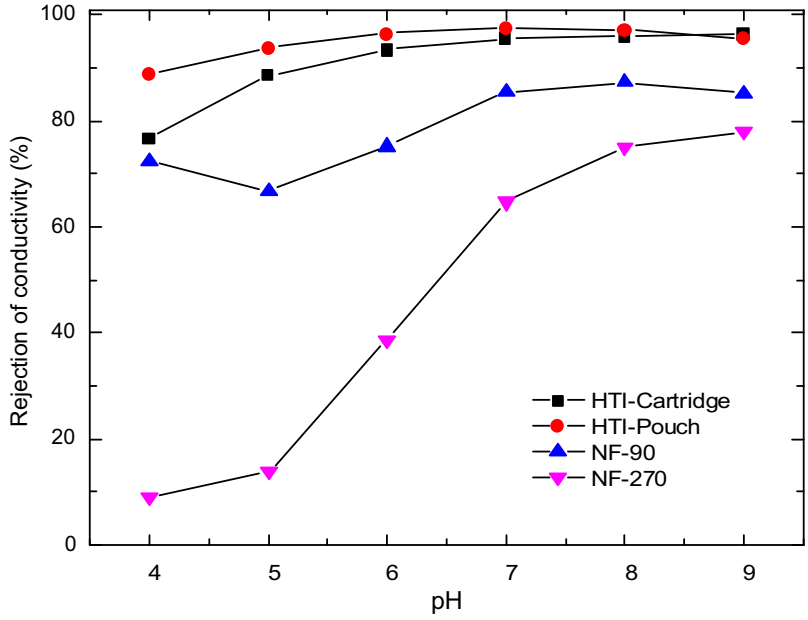

Fig. 8. Rejection of acetate as a function of different pH values of the feed. The RO experimental conditions were as follows: Initial concentration of acetate in the feed = 300 mg/L, water flux = 8 L/m^{2}h, cross- flow rate = 2 L/min, cross-flow velocity = 25 cm/s, temperature = 25 ± 1 ℃.

rejection of conductivity of the four membranes investigated in this study. Conductivity rejections by the HTI-Cartridge, HTI-Pouch, and NF-90 membranes decreased slightly as the feed solution pH decreased (Fig. 8). One exception is the NF-270 membrane which showed a dramatic decrease in conductivity rejection as the feed solution pH decreased from pH 9 to 4. Nevertheless, it is noteworthy that conductivity rejection by the NF-270 is always lower than those by the other three membranes investigated here at any given pH. This can be attributed to the large pore size of the NF-270 membrane and therefore its rejection of inorganic salts relies mostly on the electrostatic interaction mechanism [30,35]. In fact, the rejection of conductivity by the NF-270 mirrors closely its zeta potential profile (Fig. 2).

The rejections of conductivity by all four membranes presented in Fig. 8 are in good agreement with the rejection of acetate (Fig. 7). Conductivity rejections by the two FO membranes (HTI-Cartridge and HTI-Pouch) were higher than those by the two NF membranes (NF-270 and NF-90). These results cannot be explained by the membrane surface charge or pore size. The NF membranes are more negatively charged than their FO counterparts (Fig. 2). The average membrane pore sizes of these four membranes are quite comparable (Table 1). Although it can be speculated that this observation can be attributed to the much thicker active skin layer of the FO membranes compared to their NF counterparts, further investigation will be required to substantiate this hypothesis.

4. Conclusions

This study investigated the performance of two FO—namely HTI-Cartridge and HTI-Pouch—and two NF—namely NF-270 and NF-90—membranes for the removal of acetic acid from produced water. Detailed membrane characterization revealed that the NF membranes have much higher water and salt permeability (i.e. A and B values) than their FO counterparts. However, the two NF membranes could not be used in the FO mode to produce any measurable water permeate flux. Under the same operating condition, the HTI-Cartridge membrane had higher water and RSFs than those by the HTI-Pouch membrane. This difference in transport performance between the two FO membranes could be attributed to the difference in their pore size and internal structure. Similarly, due to the internal concentration polarization effect, the PRO mode resulted in higher water and RSFs than the FO mode. Acetate rejection was pH dependent in both the FO and RO modes. In addition, in the RO mode, acetate rejections by the FO membranes were higher than their NF counterparts. Results reported here suggest that FO can be a viable treatment option for the removal of dissolved organics from produced water.

Acknowledgements

We acknowledge the scholarship provided by the Libyan Government to Rajab Abousnina. Hydration Technology Innovations and Dow Chemical are thanked for the provision of membrane samples.

References

[1] N. Das, P. Chandran, Microbial degradation of petroleum hydrocarbon contaminants: An overview, Biotechnol. Res. Int. (2011) 1–13.
[2] M.A. Quddus Khan, S.M. Al-Ghais, B. Catalin, Y.H. Khan, Chapter 12 effects of petroleum hydrocarbons on aquatic animals, Develop. Earth Environ. Sci. 3 (2005) 159–185.
[3] D.L. Nghiem, T. Ren, N. Aziz, I. Porter, G. Regmi, Treatment of coal seam gas produced water for beneficial use in Australia: A review of best practices, Desalin. Water Treat. 32 (2011) 316–323.
[4] John A. Veil, Markus G. Puder, Deborah Elcock, J. Robert, J. Redweik. A White Paper Describing Produced Water from Production of Crude Oil, Natural Gas, and Coal Bed Methane, 2004 [cited 2011 20/09]. Available from: http://www.ead.anl.gov/pub/doc/ProducedWatersWP0401.pdf.
[5] S.J. Johnson, K.J. Woolhouse, H. Prommer, D.A. Barry, N. Christofi, Contribution of anaerobic microbial activity to natural attenuation of benzene in groundwater, Eng. Geol. 70(3–4) (2003) 343–349.
[6] S. Schulze, A. Tiehm, Assessment of microbial natural attenuation in groundwater polluted with gasworks residues, Water Sci. Technol. 50(5) (2004) 347–353.
[7] B.A. Bekins, I.M. Cozzarelli, G.P. Curtis, A simple method for calculating growth rates of petroleum hydrocarbon plumes, Groundwater 43(6) (2005) 817–826.
[8] B. Hendrickx, W. Dejonghe, F. Faber, W. Boënne, L. Bastiaens, W. Verstraete, E.M. Top, D. Springael, PCR-DGGE method to assess the diversity of BTEX mono-oxygenase genes at contaminated sites, FEMS Microbiol. Ecol. 55(2) (2006) 262–273.
[9] O. Atteia, C. Guillot, Factors controlling BTEX and chlorinated solvents plume length under natural attenuation conditions, J. Contamin. Hydrol. 90(1–2) (2007) 81–104.
[10] J.P. Biggerstaff, M. Le Puil, B.L. Weidow, J. Leblanc-Gridley, E. Jennings, J. Busch-Harris, K.L. Sublette, D.C. White, R.S. Alberte, A novel and *in situ* technique for the quantitative detection of MTBE and benzene degrading bacteria in contaminated matrices, J. Microbiol. Methods 68(2) (2007) 437–441.
[11] A. Fakhru'l-Razi, A. Pendashteh, L.C. Abdullah, D.R.A. Biak, S.S. Madaeni, Z.Z. Abidin, Review of technologies for oil and gas produced water treatment, J. Hazard. Mater. 170(2–3) (2009) 530–551.
[12] A. Fakhru'l-Razi, Alireza Pendashteh, Zurina Zainal Abidin, Luqman Chuah Abdullah, Dayang Radiah Awang Biak, Sayed Siavash Madaeni, Application of membrane-coupled sequencing batch reactor for oilfield produced water recycle and beneficial re-use. Bioresour. Technol. 101(18) (2010) 6942-6949.
[13] R.R. Bhave, H.L. Fleming, Removal of oily contaminants in wastewater with microporous alumina membranes, American Institute of Chemical Engineers, Symposium Series, New Membrane Materials and Processes for Separations, 84(261) (1988) 1.
[14] A.S.C. Chen, J.T. Flynn, R.G. Cook, A.L. Casaday, Removal of oil, grease, and suspended solids from produced water with ceramic crossflow microfiltration, SPE Prod. Eng. 6(2) (1991) 131–136.
[15] U. Daiminger, W. Nitsch, P. Plucinski, S. Hoffmann, Novel techniques for oil/water separation, J. Membr. Sci. 99(2) (1995) 197–203.
[16] T.Y. Cath, A.E. Childress, M. Elimelech, Forward osmosis: Principles, applications, and recent developments, J. Membr. Sci. 281(1–2) (2006) 70–87.
[17] R.L. McGinnis, M. Elimelech, Energy requirements of ammonia–carbon dioxide forward osmosis desalination, Desalination 207(1–3) (2007) 370–382.
[18] E.R. Cornelissen, D. Harmsen, K.F. de Korte, C.J. Ruiken, J.-J. Qin, H. Oo, L.P. Wessels, Membrane fouling and process performance of forward osmosis membranes on activated sludge, J. Membr. Sci. 319(1–2) (2008) 158–168.
[19] B. Mi, M. Elimelech, Organic fouling of forward osmosis membranes: Fouling reversibility and cleaning without chemical reagents, J. Membr. Sci. 348(1–2) (2010) 337–345.
[20] A. Achilli, T.Y. Cath, E.A. Marchand, A.E. Childress, The forward osmosis membrane bioreactor: A low fouling alternative to MBR processes, Desalination 239(1–3) (2009) 10–21.
[21] C.R. Martinetti, A.E. Childress, T.Y. Cath, High recovery of concentrated RO brines using forward osmosis and membrane distillation, J. Membr. Sci. 331(1–2) (2009) 31–39.
[22] J.R. McCutcheon, M. Elimelech, Influence of membrane support layer hydrophobicity on water flux in osmotically driven membrane processes, J. Membr. Sci. 318(1–2) (2008) 458–466.
[23] L.D. Nghiem, A.I. Schaffer, M. Elimelech, Nanofiltration of hormone mimicking trace organic contaminants, Sep. Sci. Technol. 40(13) (2005) 2633–2649.
[24] M. Xie, L.D. Nghiem, W.E. Price, M. Elimelech, Comparison of the removal of hydrophobic trace organic contaminants by forward osmosis and reverse osmosis, Water Res. 46(8) (2012) 2683–2692.
[25] H.T. Innovations. A World Leader in Water Technologies, 2010 [cited 15/3/2012]. Available from: http://www.hti-water.com/.
[26] T.Y. Cath, M. Elimelech, J.R. McCutcheon, R.L. McGinnis, A. Achilli, D. Anastasio, A.R. Brady, A.E. Childress, I.V. Farr, N. T. Hancock, J. Lampi, L.D. Nghiem, M. Xie, N.Y. Yip, Standard methodology for evaluating membrane performance in osmotically driven membrane processes, Desalination 312 (2013) 31–38.
[27] L.D. Nghiem, A.I. Schäfer, M. Elimelech, Removal of natural hormones by nanofiltration membranes: Measurement, modeling, and mechanisms, Environ. Sci. Technol. 38(6) (2004) 1888–1896.
[28] S.G.J. Heijman, A.R.D. Verliefde, E.R. Cornelissen, G. Amy, J. C. van Dijk, Influence of natural organic matter (NOM) fouling on the removal of pharmaceuticals by nanofiltration and activated carbon filtration, Water Sci. Technol.: Water Supply 7(4) (2007) 17.
[29] A.R.D. Verliefde, E.R. Cornelissen, S.G.J. Heijman, J.Q.J.C. Verberk, G.L. Amy, B. Van der Bruggen, J.C. van Dijk, The role of electrostatic interactions on the rejection of organic solutes in aqueous solutions with nanofiltration, J. Membr. Sci. 322(1) (2008) 52–66.
[30] L.D. Nghiem, A.I. Schafer, M. Elimelech, Role of electrostatic interactions in the retention of pharmaceutically active contaminants by a loose nanofiltration membrane, J. Membr. Sci. 286(1–2) (2006) 52–59.
[31] Nathan T. Hancock, William A. Phillip, Menachem Elimelech, A.T.Y. Cath, Bidirectional permeation of electrolytes in osmotically driven membrane processes, Environ. Sci. Technol. 45(24) (2011) 10642–10651.
[32] Jeffrey R. McCutcheon, Robert L. McGinnis, Elimelech Menachem, Desalination by ammonia carbon dioxide forward osmosis: Influence of draw and feed solution concentrations on process performance, J. Membr. Sci. 278(1–2) (2006) 114–123.
[33] C. Kim, S. Lee, H.K. Shon, M. Elimelech, S. Hong, Boron transport in forward osmosis: Measurements, mechanisms, and comparison with reverse osmosis, J. Membr. Sci. 419–420 (2012) 42–48.
[34] M. Xie, W.E. Price, L.D. Nghiem, Rejection of pharmaceutically active compounds by forward osmosis: Role of solution pH and membrane orientation, Sep. Purif. Technol. 93 (2012) 107–114.
[35] L.D. Nghiem, A.I. Schäfer, M. Elimelech, Pharmaceutical retention mechanisms by nanofiltration membranes, Environ. Sci. Technol. 39(19) (2005) 7698–7705.